

Bit Error Rate Evaluation of Delay Time Control Scheme for Reverse Channel on Orthogonal Coding Multi-Carrier CDMA*

Souichi WATANABE[†], Takuro SATO[†], Masakazu SENGOKU^{††}, and Takeo ABE[†], Members

SUMMARY This paper describes a delay control scheme for synchronous detection of an orthogonal coding multi-carrier CDMA (Code Division Multiple Access) system. The delay control scheme estimates transmission timing of data from each mobile station. At a base station, delay time is obtained by detecting phase shift value of the preamble signal from each mobile station. The estimated transmission timing information is sent from base station to each mobile station and the mobile station then adjusts its transmission timing. Simulation results clarified that Bit Error Rate (BER) is 2.5×10^{-3} at 19 dB of E_b/N_0 under conditions of 29.4 msec initial delay time, 32 kbit/sec data rate, 16 subchannels and 100 Hz of fading frequency.

key words: multi-carrier, CDMA, delay time control

1. Introduction

Recently, OFDM (Orthogonal Frequency Division Multiplexing) scheme has been studied for application to broadcast and personal communication systems [1]–[4]. OFDM is characterized as robust for radio environments because of low data rate of subchannel signals. Authors have been studying an orthogonal coding multi-carrier CDMA. The multi-carrier CDMA multiplexes subscribers' data which are spread by Walsh orthogonal codes in each subchannel in order to increase system capacity [5]–[7]. In the orthogonal coding multi-carrier CDMA, a base station synchronously transmits the orthogonal spread data on the forward channel. Each mobile station detects subscribers' data utilizing synchronous timing. On the reverse channel each mobile station asynchronously transmits subscriber's data and the base station detects data from each subscriber with different timing. The asynchronous received timing at the base station causes Inter-Symbol Interference (ISI) which degrades the orthogonal relation between each subscribers' data. Therefore, the ISI degrades BER performance on the reverse channel in comparison with the forward channel. A delay equalization method has been proposed to reduce the ISI for TDMA

(Time Division Multiple Access) systems [8], [9]. However, this delay equalization is difficult to apply for the orthogonal coding multi-carrier CDMA on the reverse channel, since each subscriber's data is multiplexed by CDM (Code Division Multiplexing) and each data stream is influenced by different propagation paths and different fading characteristics. The delay time control scheme adjusts the transmission timing of each mobile station to detect the subscriber's data at the same timing for reverse channel. The base station estimates the transmission delay time of each mobile station using the preamble signals which are sent from the mobile stations to the base station. The estimated delay time information is sent from the base station to each mobile station to control the transmission timing. The delay time control of reverse channel results in same BER for both channels.

Section two describes the system configuration of orthogonal coding multi-carrier CDMA. Section three describes analysis results of ISI. Section four describes the delay time control. Section five describes simulation results under white Gaussian noise and fading environment.

2. System Configuration

Figure 1 shows the configuration of the orthogonal coding multi-carrier CDMA. Figure 2 gives a time chart of baseband signals of a reverse channel transmitter. At a transmitter of a mobile station, input data D_m from subscriber m converts to data $D_{m,k}$ of subchannel k through a S/P (Serial/Parallel converter). Each subchannel data stream is spread by the Walsh orthogonal code $W_m^{(n)}$ which is assigned for each subscriber and Base Station Identification Sequence ($BIS^{(n)}$), where $BIS^{(n)}$ is pseudo random sequence.

The chip data of subchannel k of subscriber m is shown as follows:

$$X_{m,k}^{(n)} = D_{m,k} \oplus W_m^{(n)} \oplus BIS^{(n)} \quad (1)$$

where \oplus denotes exclusive-OR operation and n means chip time. Each chip of subchannel k satisfies the following relation:

Manuscript received November 30, 1996.

Manuscript revised February 20, 1997.

[†]The authors are with the Niigata Institute of Technology, Kashiwazaki-shi, 945-11 Japan.

^{††}The author is with the Niigata University, Niigata-shi, 950-21 Japan.

*This paper was presented in part at the IEICE Multi-Dimensional Mobile Communications '96, Seoul, Korea, July 18-20, 1996

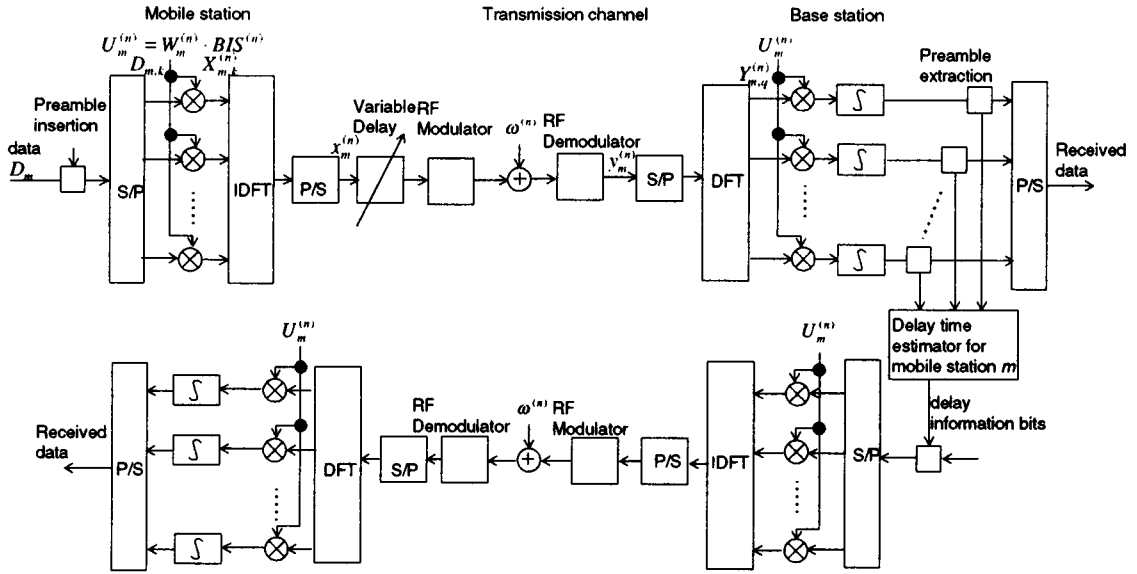


Fig. 1 Configuration of delay time control.

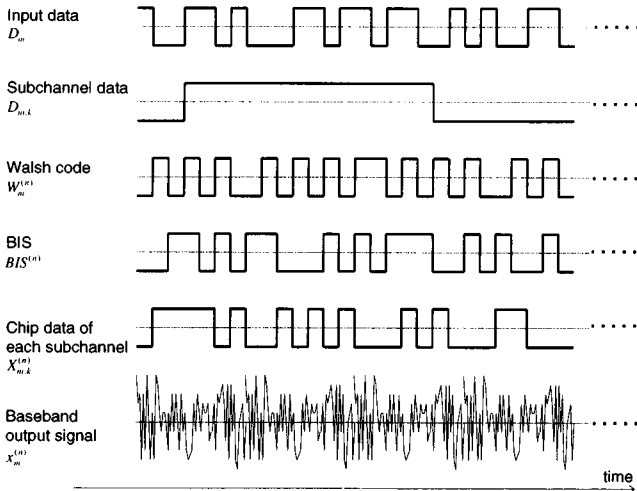


Fig. 2 Time chart of spread data and baseband output signal for transmitter.

$$\sum_{n=0}^{N-1} X_{m,k}^{(n)} \cdot X_{m',k}^{(n)} = \begin{cases} N, & m = m' \\ 0, & m \neq m' \end{cases} \quad (2)$$

Subchannel chip data is converted to the baseband transmission signal through IDFT (Inverse Discrete Fourier Transformation) and P/S (Parallel Serial converter), where the number of samples of IDFT frame are N and duration is T_c .

Figure 3 shows a spectrum of the transmitting baseband signal. The set of the transmitting signals satisfies the orthogonal relations every $1/T_c$. The mobile station transmits a preamble signal in order to estimate the delay time between the mobile station and the base station. The preamble signal becomes a delta function when input data D_m is one. The mobile station transmits the preamble signal with the synchronized timing

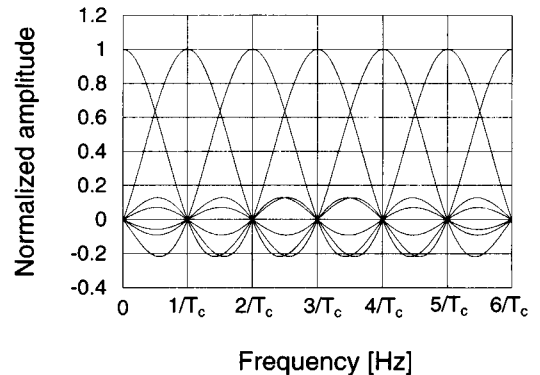


Fig. 3 Spectrum of baseband output signal.

for the received data from the base station. At a receiver of the base station, the received signal is converted to subchannel data through Discrete Fourier Transformation (DFT). The number of DFT samples are N and the duration of DFT frame is T_c . The subchannel data is obtained by despreading with BIS and Walsh orthogonal code for each subchannel. The subchannel signals are converted to subscribers' data through the Parallel/Serial converter (P/S). Even when the transmitting timing of mobile station is synchronized with the received forward channel signal, the base station detects the data at asynchronous timing due to the distance between the mobile station and the base station. The receiver calculates the delay time from the received preamble signal in a delay time estimator. The estimated delay information is input to the forward channel data. At a base station transmitter, using the relation of Eq. (2), chip data of each subchannel is multiplexed by Code Division Multiplexing. Since all subscribers' data are transmitted synchronously for forward chan-

nel, ISI doesn't appear in subchannel if we ignore the carrier offset and the multi-path delay. At a receiver of the mobile station, all multiplexed data are detected synchronously. The detail of delay control scheme is described in Sect. 4.

3. Analysis of Inter-Symbol Interference and BER Performance

This section analyzes the degradation of BER performance caused by ISI. This analysis ignores the carrier offset and the multi-path delay between the transmitter and the receiver. The base station asynchronously detects the signals from the mobile stations. Timing difference of the received signal from each mobile station gives the ISI in chip signal.

Figure 4 shows the received chip at the base station and it also shows the decision timing of the received chip. The previous chip signal gives distortion in the present chip signal because of decision timing error. The decision timing error causes distortion in the subchannel. The distortion is evaluated as the ISI. For simplified analysis, we focus only subscriber m . The OFDM transmission signal of the mobile station m is shown as follows:

$$x_m^{(n)} = \sqrt{E_m/N} \sum_{k=0}^{N-1} X_{m,k}^{(n)} e^{j2\pi kp/N} \quad (3)$$

where $X_{m,k}^{(n)}$ is subchannel data, k is subchannel number, $\sqrt{E_m}$ is average transmitting voltage, N is number of subchannels and p is sampling time which is normalized by T_c/N (T_c is chip duration). It is assumed that the number of subchannels is the same as number of mobiles in a cell. When the timing difference is Δ_m , the analyzed region is divided from 0 to Δ_m and from Δ_m to T_c . The received signal from subchannel k of mobile station m is shown as follows:

$$y_m^{(n)} = \begin{cases} \sqrt{E_m/N} X_{m,k}^{(n-1)} e^{j2\pi k(p-\Delta_m \cdot N/T_c)/N} \\ \quad + \omega_q^{(n)}, & 0 \leq p < \Delta_m \cdot N/T_c \\ \sqrt{E_m/N} X_{m,k}^{(n)} e^{j2\pi k(p-\Delta_m \cdot N/T_c)/N} \\ \quad + \omega_q^{(n)}, & \Delta_m \cdot N/T_c \leq p < N \end{cases} \quad (4)$$

where $\omega_q^{(n)}$ is thermal noise. The received signal is converted to subchannel signal through S/P and DFT. The received subchannel signal of mobile station m is shown as follows:

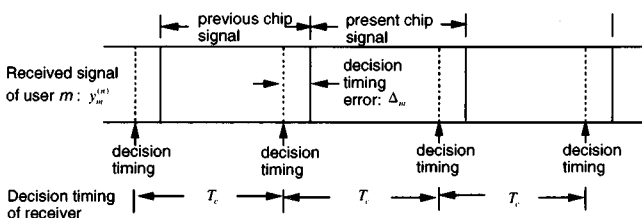


Fig. 4 Received chip signal at base station.

$$Y_{m,q}^{(n)} = \sum_{p=0}^{N-1} y_m^{(n)} e^{-j2\pi qp/N} \quad (5)$$

where q denotes the receiving subchannel number. ISI is appeared in subchannel signal due to delay time Δ_m . ISI is shown as follows:

$$\begin{aligned} I_{m,q}^{(n)} &= \sum_{\substack{k=0 \\ k \neq q}}^{N-1} \sum_{p=0}^{N-1} y_{m,k}^{(n)} e^{-j2\pi qp/N} \\ &= \sqrt{E_m/N} \sum_{k=1}^{N-1} \\ &\quad [X_{m,k}^{(n-1)} \sum_{p=0}^{\Delta-1} \cos(2\pi(k-q)(p-\Delta)/N) \\ &\quad + X_{m,k}^{(n)} \sum_{p=\Delta}^{N-1} \cos(2\pi(k-q)(p-\Delta)/N)] \end{aligned} \quad (6)$$

where Δ is discrete value of Δ_m which is normalized by sampling rate N/T_c of DFT. Considering the interference from other subscribers, the received chip of mobile station m is shown as follows:

$$Y_{m,q}^{(n)} = X_{m,q}^{(n)} + \sum_{l=0}^{N-1} I_{l,q}^{(n)} + \omega_q^{(n)} \quad (7)$$

where $X_{m,q}^{(n)}$ is desired signal, $I_{l,q}$ is the interference from mobile station l and $\omega_q^{(n)}$ is thermal noise of subchannel q . BER is obtained by error function. It is shown as follows:

$$P_E = \frac{1}{2} \operatorname{erfc} \left[\sqrt{E_m / \left\{ \sum_{l=0}^{N-1} \langle \|I_{l,q}^{(n)}\|^2 \rangle + \langle \|\omega_q^{(n)}\|^2 \rangle \right\}} \right] \quad (8)$$

where $\langle \|\cdot\| \rangle$ denotes power. BER can be simplified further by upper bounding due to Chernoff limitation [10]: It is shown as follows:

$$\begin{aligned} P_E &= P_r \left(\sum_{n=0}^{N-1} Y_{m,q}^{(n)} \cdot U_m^{(n)} > 0 \mid D_{m,q} = -1 \right) \\ &< E \left[e^{\rho \sum_{n=0}^{N-1} Y_{m,q}^{(n)} \cdot U_m^{(n)}} \right] \\ &< e^{-\rho N \sqrt{E_m/N}} \\ &\quad \cdot \prod_{n=0}^{N-1} \left[\left(\prod_{l=0}^{N-1} E[e^{\rho I_{l,q}^{(n)} \cdot U_m^{(n)}}] \right) E[e^{\omega_q^{(n)}} \cdot U_m^{(n)}] \right] \end{aligned} \quad (9)$$

where $\rho > 0$ and $U_m^{(n)} = BIS^{(n)} \cdot W_m^{(n)}$.

$$E[e^{\rho I_{l,q}^{(n)} \cdot U_m^{(n)}}] = e^{\langle \|I_{l,q}^{(n)}\|^2 \rangle \rho^2 / 4} \quad (10)$$

$$P_E < \min_{\rho > 0} e^{-N \{ \rho \sqrt{E_m/N} - \rho^2 I_0 / 4 \}} \quad (11)$$

where

$$I_0 = \langle \|\omega_q^{(n)}\|^2 \rangle + \sum_{l=0}^{N-1} \langle \|I_{l,q}^{(n)}\|^2 \rangle$$

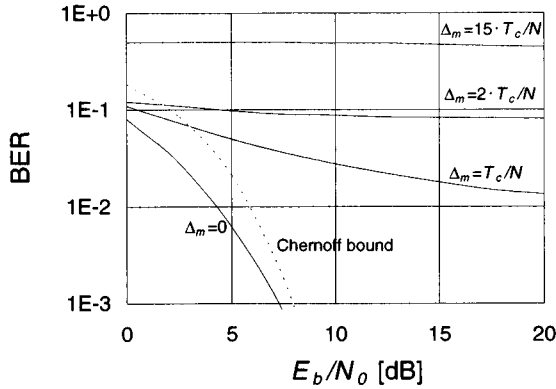


Fig. 5 Analysis results of BER versus E_b/N_0 under white Gaussian noise channel.

Assuming that the probability distribution function of $\omega_q^{(n)}$ and $I_{l,q}^{(n)}$ are Gaussian, the value of ρ which minimize Eq. (11) is shown as follows:

$$\rho = 2\sqrt{E_m/N}/I_0 \tag{12}$$

Inserting Eq. (12) to (11) and multiplying improving factor (1/2), the upper bound of BER is shown as follows:

$$P_E < \frac{1}{2} \cdot e^{-E_m/I_0} \tag{13}$$

Figure 5 shows an analysis result of BER versus E_b/N_0 as a parameter of delay time Δ_m of the orthogonal coding multi-carrier CDMA. It also shows the upper limitation of BER calculated from Eq. (13). In the analysis, the number of subchannels N is 16 and chip duration T_c is 31.25 msec ($= 1/32$ kchip/sec). These parameters are the same as simulation parameters in Sect. 5. These results show that a small delay time Δ_m degrades BER performance.

4. Delay Time Control

Since the mobile station transmits the preamble data which is all “one,” the baseband output signal becomes delta function $N\delta(p)$ after IDFT. The analysis is done assuming that the power control is perfect and non-linearity of an amplifier is ignored.

Figure 6 shows the received preamble signal at the base station. The hatched preamble signal shows synchronous point. Other subscriber’s preamble signals are detected with delay time Δ_m . The Delay time of each mobile station is estimated when all subscribers’ preamble signals are detected within same DFT sampling frame T_c . This is the acceptable delay time. The preamble signal of mobile station m is shown as follows:

$$x_m^{(n)} = \delta(p) \cdot U_m^{(n)} \tag{14}$$

where coefficient $\sqrt{NE_m}$ is ignored in this section for simplicity. At the base station, the receiving signal is shown as follows:

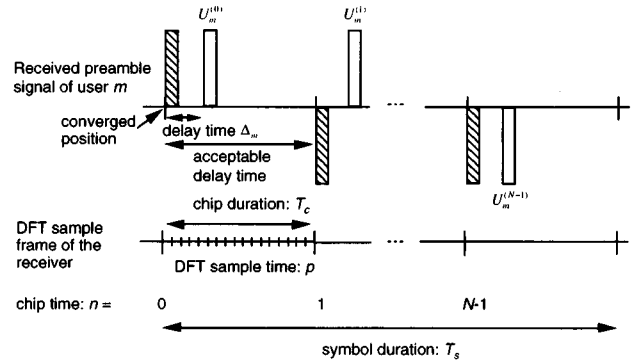


Fig. 6 Received preamble signal at base station.

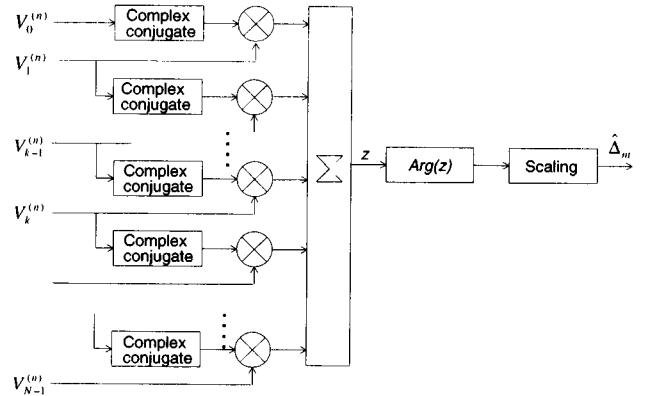


Fig. 7 Configuration of delay time estimator.

$$v(p) = \sum_{m=0}^{N-1} U_m^{(n)} \delta(p - \Delta_m) + \omega(p) \tag{15}$$

where $\omega(p)$ is thermal noise. The chip signal on the subchannel k through DFT is shown as follows:

$$V_k^{(n)} = U_m^{(n)} e^{-j2\pi k \Delta_m / T_c} + \omega_k^{(n)} \tag{16}$$

where $\omega_k^{(n)}$ is thermal noise of subchannel k .

Figure 7 shows a configuration of the delay time estimator. It calculates the delay time of each subscriber from received preamble signal. The phase difference of the preamble signals between neighbor subchannels is obtained as follows:

$$\begin{aligned} z &= \sum_{k=1}^{N-1} V_k^{(n)} (V_{k-1}^{(n)})^* \\ &= (N-1)e^{-j2\pi \Delta_m / T_c} \\ &\quad + \sum_{k=1}^{N-1} (U_m^{(n)} e^{-j2\pi k \Delta_m / T_c} \cdot \omega_{k-1}^{(n)*} \\ &\quad + U_m^{(n)} e^{j2\pi (k-1) \Delta_m / T_c} \cdot \omega_k^{(n)} \\ &\quad + \omega_k^{(n)} \omega_{k-1}^{(n)*}) \end{aligned} \tag{17}$$

where * denotes complex conjugate. The results show the accuracy of delay time estimation degrades due to increase of the noise $\omega_k^{(n)}$ and $\omega_{k-1}^{(n)}$. If the noise term of Eq. (17) is small, delay time Δ_m is evaluated as $\hat{\Delta}_m$ from the phase angle of z . It is shown as follows:

$$\hat{\Delta}_m = -\frac{T_c \cdot \arg(z)}{2\pi} \quad (18)$$

If the delay time difference is in a chip duration T_c , there is no interference between the subscribers. The base station transmits the delay time information to each mobile station. The mobile station controls the transmission timing of data in accordance with the delay time information.

5. Simulation Results

This section describes the simulation results of the orthogonal coding multi-carrier CDMA with delay time control shown in Figs. 1 and 7. System parameters of

Table 1 System parameters of simulation.

Parameter	Value
Data rate	32 kbit/sec
Symbol rate of subchannel	2 kbit/sec
Chip rate	32 kchip/sec
Number of subchannels: N	16
Number of subscribers: N	16
Number of Walsh orthogonal codes	16
PN sequence of BIS	$2^{15} - 1$

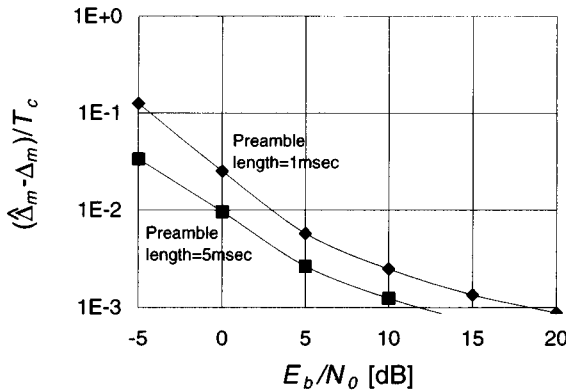


Fig. 8 Estimated delay time error versus E_b/N_0 under white Gaussian noise channel as parameters of preamble length (Preamble length are 1 and 5 msec).

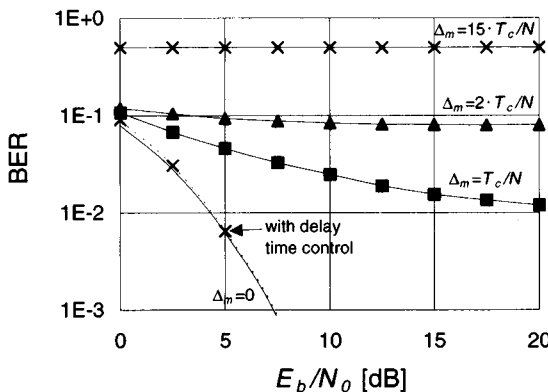


Fig. 9 Simulation results of BER versus E_b/N_0 under white Gaussian noise channel as parameters of delay time.

the simulations are shown in Table 1. In this simulation, the transmission time of the forward channel is ignored.

5.1 Simulation Results under White Gaussian Noise

Figure 8 shows the mean value of estimation error versus E_b/N_0 as a parameter of preamble length under a white Gaussian noise environment. This result shows, when the preamble length is 1 msec, more than 2 dB of E_b/N_0 is required in order to satisfy the 0.02 of estimation error, where the 0.02 is the assumed value of the threshold level of convergence state. On the other hand, it is more than -2 dB of E_b/N_0 when the preamble length is 5 msec. Therefore, a longer preamble length decreases estimation error and improves BER performance.

Figure 9 shows the simulation results of the BER performance versus E_b/N_0 as parameters of delay time for the reverse channel. White Gaussian noise is added to the reverse channel. The figure shows that initial conditions of T_c/N (2 msec), $2T_c/N$ (3.9 msec) and $15T_c/N$ (29.3 msec) of delay time from the mobile station to base station. The dashed line shows BER performance with delay time control whose initial delay times are T_c/N , $2T_c/N$ and $15T_c/N$. The simulation results show that the performance of BER improves from 4.6×10^{-2} (initial delay time = T_c/N), 9.4×10^{-2} ($2T_c/N$) and 0.5 ($15T_c/N$) to 6.5×10^{-3} under the condition of 5 dB of E_b/N_0 using the delay time control scheme.

5.2 Simulation Results under Fading Condition

Figure 10 shows mean value of estimation error versus E_b/N_0 as parameters of preamble length and fading frequency. This result shows, when the preamble length is 1 msec, more than 19 dB of E_b/N_0 is required in order to satisfy the 0.02 of estimation error for both 50 and 100 Hz of fading frequencies. When the preamble length is 5 msec, about 5 dB of E_b/N_0 is required. This

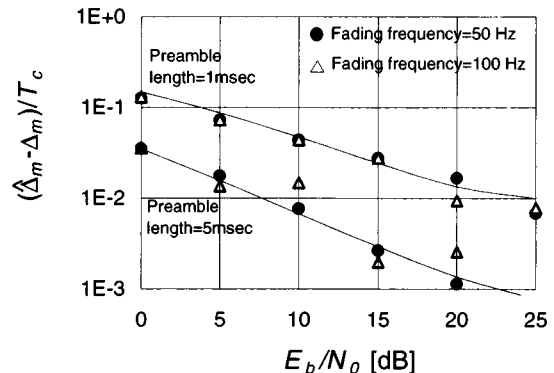


Fig. 10 Estimated delay time error versus E_b/N_0 under fading channel as parameters of preamble length and fading frequency (preamble length are 1 and 5 msec and fading frequencies are 50 and 100 Hz).

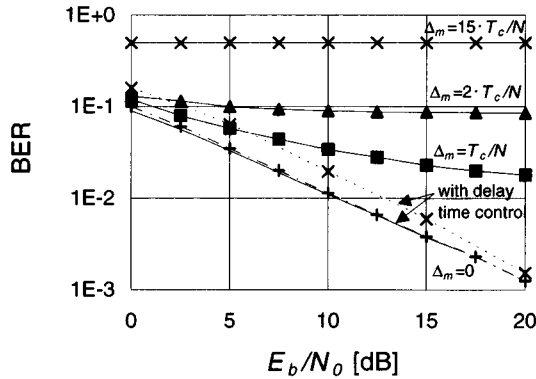


Fig. 11 Simulation results of BER versus E_b/N_0 under fading channel as a parameter of delay time (fading frequency is 50 Hz). Preamble length = 1 ms — — —, Preamble length = 5 ms - - - - -

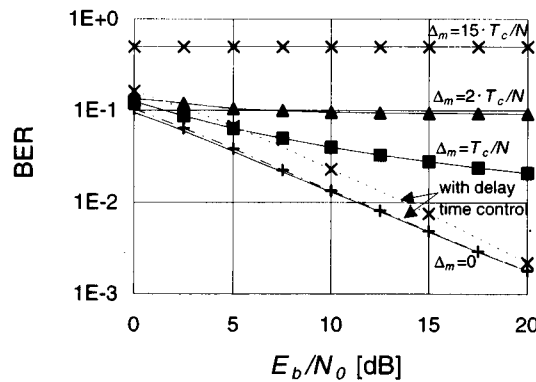


Fig. 12 Simulation results of BER versus E_b/N_0 under fading channel as a parameter of delay time (fading frequency is 100 Hz). Preamble length = 1 ms — — —, Preamble length = 5 ms - - - - -

result shows the delay time estimation is less affected by fading frequency in a selected parameter range.

Figures 11 and 12 show the simulation results of the BER performance versus E_b/N_0 as parameters of delay time for reverse channel in the fading environment. The fading frequencies are 50 Hz and 100 Hz respectively which correspond to 54 and 108 km/h of moving speed at 1 GHz carrier frequency. The dashed and dotted lines show BER performance with delay time control whose preamble length is 1 msec and 5 msec respectively. For the case of 50 Hz of the fading frequency, BER improves from 1.8×10^{-2} (initial delay time = T_c/N), 9.0×10^{-2} ($2T_c/N$) and 0.5 ($15T_c/N$) to 2.0×10^{-3} (preamble length = 1 msec) and 1.6×10^{-3} (preamble length = 5 msec) under the condition of 19 dB of E_b/N_0 using the delay time control scheme. For the case of 100 Hz of the fading frequency, BER improves from 2.1×10^{-2} (initial delay time = T_c/N), 9.5×10^{-2} ($2T_c/N$) and 0.5 ($15T_c/N$) to 2.5×10^{-3} (preamble length = 1 msec) and 2.0×10^{-3} (preamble length = 5 msec) under the condition of 19 dB of E_b/N_0 using the delay time control scheme. Since 50 and 100 Hz of the

fading frequencies are less than 1/10 of subchannel data rate 2 kbit/sec, the ISI does not affect degradation of the BER performance. The simulation results show that the BER performance under the 50 Hz of fading frequency is slightly better than the performance under the 100 Hz fading frequency because the subchannel data rate is closer to the 100 Hz fading frequency. If the fading frequency become close to the data rate, the correlation

value $\sum_{n=0}^{N-1} X_{m,k}^{(n)} \cdot X_{m',k}^{(n)} e^{j2\pi f_d n T_c}$ do not become zero, where f_d is fading frequency. The ISI degrades the BER performance. In order to maintain stable delay time control, the interval of preamble insertion must satisfy the condition $(\hat{\Delta}_m - \Delta_m)/T_c > vT_p/(cT_c)$, where v , T_p and c are moving speed of mobile station, preamble interval and light speed respectively. We set the threshold level of convergence state as $(\hat{\Delta}_m - \Delta_m)/T_c = 0.02$ in above simulations. Assuming that moving speed v is 100 km/h, the condition clarifies that the delay time control system is stable when T_p is less than 6.7 sec.

6. Conclusion

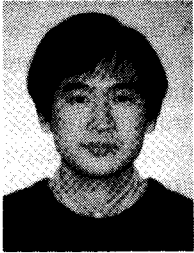
This paper describes a delay time control scheme for orthogonal coding multi-carrier CDMA. Simulation results clarify the range of the acceptable delay time and the required preamble length. The delay time control scheme is very effective to reduce the transmission delay time. The adoption of the delay control scheme improves the BER performance for the reverse channel. In this system, the preamble signal is used to estimate the timing of the receiving signal. In this paper, the practical design values are used to evaluate the system performance. As the results of analysis and the computer simulation, this paper clarified the effectiveness of the usage of the delay time control scheme on the orthogonal coding multi-carrier CDMA. We will continue to study the proposed delay control scheme with interference noise from neighbor cells and sectors and the distribution of mobile stations within a cell.

References

- [1] M. Alard and R. Lassalle, "Principles of modulation and channel coding for digital broadcasting for mobile receivers," EBU Review-technical, no.224, pp.169-189, Aug. 1987.
- [2] L. Vandendorpe, "Multitone spread spectrum multiple access communications system in a multipath Rician fading channel," IEEE Trans. Veh. Technol., vol.44, no.2, pp.327-337, May 1995.
- [3] E.A. Sourour and M. Nakagawa, "Performance of orthogonal multicarrier CDMA in a multipath fading channel," IEEE Trans. commun. vol.44, no.3, March 1996.
- [4] T. Muller and R. Grunheid, "Comparison of detection algorithms for OFDM-CDMA in broadband Rayleigh fading," IEEE VTC, vol.2, pp.835-838, July 1995.
- [5] T. Sato and S. Watanabe, "Orthogonal coding multi-carrier CDMA scheme," 1, Technical report, IEICE Multi-

dimensional Mobile Information Networks '96, pp.1-6, Matumoto Japan, April 1996.

- [6] T. Sato, S. Watanabe, and T. Abe, "Synchronization analysis of orthogonal coding multi-carrier CDMA under multipath fading," A3-1, International Technical Conference on Circuits/Systems, Computers and Communications '96, Seoul Korea, pp.46-49, July 1996.
- [7] T. Sato, S. Watanabe, and T. Abe, "Modulation and demodulation characteristic of orthogonal coding multi-carrier CDMA scheme," Technical report A-VII .3, IEICE Multi-Dimensional Mobile Communications '96, pp.740-744, Seoul Korea, July 1996.
- [8] R.D. Avella, L. Moreno, and M. Sant Agostino, "Adaptive Equalization in TDMA radio system," Proc. IEEE 37th, IEEE VTC, pp.385-392, June 1987.
- [9] S.L. Marple, Jr., "Efficient least squares FIR system identification," IEEE Trans. Acoust., Speech & Signal Process., vol.ASSP-29, pp.62-73, Feb. 1981.
- [10] A.J. Viterbi "CDMA Principles of Spread Spectrum Communication," Addison Weseley, 1995, ISBN 0-201-63374-4 pp.78-84.



Souichi Watanabe was born in Japan 1969. He received the B.S. (EE) and M.S. (EE) degrees from Niigata University in 1991 and 1993, respectively. He is presently working in Niigata Institute of Technology, Japan. His current research interest is multi-carrier communication systems.



Takuro Sato was born in Niigata prefecture, Japan, On January 16, 1950. He received the B.E. and Ph.D. degrees in electronics engineering from Niigata University, in 1973 and 1994, respectively. He was with Research and Development Laboratories, Oki Electric Industry Co., Ltd., Tokyo, Japan, on PCM transmission equipment, mobile telephone, mobile data transmission, nonlinear system and neural network. He is currently Professor,

Department of Information and Electronics Engineering, Niigata Institute of Technology. His current research is in personal communication systems, digital signal processing and automatic control system.



Masakazu Sengoku received the B.E. degree in electrical engineering from Niigata University, Niigata, Japan, 1967 and the M.E. and Ph.D. degrees from Hokkaido University in 1969 and 1972, respectively. In 1972, he joined the staff at Department of Electronic Engineering, Hokkaido University as a Research Associate. In 1978, he was an Associate Professor at Department of Information Engineering, Niigata University, where he is presently

a Professor. His research interests include network theory, graph theory, transmission of information and mobile communications. He received the Paper Awards from IEICE in 1992 and 1996, and IEEE ICNNSP Best Paper Award in 1996. He was 1995 Chairman of IEICE Technical Group on Circuits and Systems (TG-CAS). He is a senior member of IEEE, a member of the Information Processing Society of Japan and Japan Society for Industrial and Applied Mathematics.



Takeo Abe received the B.E. and Dr.Eng. degrees from Tokyo Institute of Technology in 1949 and 1966, respectively. From 1950 to 1959, he was a Research Scientist at the Electrotechnical Laboratory, Tokyo. From 1962 to 1966 he was an Associate Professor at Tokyo Institute of Technology. From 1966 to 1991 he was a Professor at Niigata University. From 1991 to 1995 he was a Professor at Chiba Institute of Technology. He is now

President of Niigata Institute of Technology. He received the Paper Award from IEICE in 1992 and IEEE ICNNSP Best Paper Award in 1996. His interests are in the field of electromagnetic theory, transmission of information and network theory. He is a member of IEEE.